

Anomalies of high-frequency magnetic properties and new orientational transitions in HoFeO₃

A. M. Balbashov, G. V. Kozlov, S. P. Lebedev, A. A. Mukhin,
A. Yu. Pronin, and A. S. Prokhorov

Institute of General Physics, USSR Academy of Sciences

(Submitted 20 September 1988)

Zh. Eksp. Teor. Fiz. **95**, 1092–1107 (March 1989)

The high-frequency magnetic properties of the orthoferrite HoFeO₃ have been investigated in the frequency range 70–800 GHz at $T = 4.2$ –300 K. The transmission spectra reveal two AFMR modes (quasiferromagnetic and quasi-antiferromagnetic) and two modes due to electronic transitions inside the ground quasidoublet of the Ho³⁺ ions (R modes). The temperature dependences of the resonance frequencies, of the line widths, and of the mode contributions to the static magnetic permeabilities have been obtained. These dependences have anomalies at $T_1 = 58 \pm 2$ K, $T_2 = 51 \pm 1$ K, and $T_3 = 39 \pm 2$ K. It is shown that a new Γ_{12} canted phase is realized in HoFeO₃ in the interval T_3 – T_2 , and that spin reorientation is effected in the form of three phase transitions (Γ_4 – Γ_{24} – Γ_{12} – Γ_2) rather than the two (Γ_4 – Γ_{24} – Γ_2) heretofore assumed. A theoretical analysis and a numerical calculation of the frequencies, linewidths, and mode contributions describe well the experiment and yield the parameters of the magnetic interactions in HoFeO₃. Important features of the dynamics of the investigated phase transitions are a strong interaction (hybridization) of the AFMR and R modes and the presence of soft modes of various types.

I. INTRODUCTION

The magnetic properties of rare-earth orthoferrites [RFeO₃, where R is a rare-earth ion (REI)], which are weak ferromagnets of rhombic symmetry, are known to depend substantially on the type of the REI (Ref. 1). This is particularly strongly manifested in the dynamic magnetic properties, particularly for orientational phase transitions (OPT).^{2–16} Thus, the behavior of the antiferromagnetic-resonance (AFMR) frequencies of the Fe-subsystem in various orthoferrites can differ qualitatively even for OPT of one and the same type (Refs. 3, 5, 7–9, 11, 13, 14). The apparent reason is the interaction of the AFMR modes with the rare-earth modes caused by electronic transitions within the ground multiplet of the REI, which is split in the crystal and bulk fields. Recognizing that the cause of the spin reorientation in orthoferrites is exchange interaction of the Fe and R subsystems,¹ considerable interest attaches to investigations of the behavior and interaction of the corresponding resonance modes of these subsystems. At present, however, there are few investigations of these questions.

A convenient object for this purpose is the orthoferrite HoFeO₃ in which, according to optical-research^{17–19} data and our first results,¹³ the energy of the splitting of the ground quasidoublet of the Ho³⁺ ion is located directly in the AFMR frequency region. This orthoferrite is of interest also from another point of view. It has been assumed (e.g., Refs. 1 and 20), that in HoFeO₃ the antiferromagnetism vector \mathbf{G} of the Fe subsystem is spontaneously reoriented at $T \approx 50$ –60 K in the ac plane from the a axis (the $\Gamma_4(G_x F_z)$ phase) to the c axis ($\Gamma_2(G_x F_x)$ phase) via the canted phase $\Gamma_{24}(G_{z,x} F_{x,z})$. Our first spectroscopic investigations¹³ of HoFeO₃, however, have revealed features typical not only of this phase transition (PT), but also typical of another PT, the Morin-type transition in DyFeO₃ (Ref. 1), which is characterized by reorientation of the vector \mathbf{G} to the b axis and vanishing of the weakly ferromagnetic moment \mathbf{F} . This

is attested to also by the results of investigations²¹ of the mixed compound Ho_{0.5}Dy_{0.5}FeO₃.

The aim of the present study was an exhaustive investigation of the high-frequency properties of HoFeO₃ in the submillimeter band and of the dynamics of the OPT in this orthoferrite, and also a search for the reorientation connected with the rotation of the vector \mathbf{G} from the ac plane to the b axis.

II. EXPERIMENTAL DATA AND DISCUSSION

The investigated HoFeO₃ single crystals were grown by float zoning with radiative heating.²² The samples cut from the initial ingot were a -, b -, and c -cut plane-parallel slabs with transverse dimensions ≈ 10 mm and thickness ≈ 1 mm. An “Epsilon” backward-wave-oscillator submillimeter spectrometer²³ was used to measure the transmission spectra $T(\nu)$ of the HoFeO₃ slabs, with frequency scanning in the range $\nu = 70$ –800 GHz in a zero external field at $T = 4.2$ –300 K. The measurements were performed for all three orientations of the high-frequency magnetic field \mathbf{h} ($\mathbf{h} \parallel \mathbf{a}, \mathbf{b}, \mathbf{c}$) by a standard procedure used by us many times to study the spectra of other orthoferrites (see, e.g., Ref. 10).

We observed altogether four absorption lines in the transmission spectra. Two of them, quite narrow ($\Delta\nu/\nu < 10^{-2}$) and observable in the entire investigated temperature range, constitute the quasiferromagnetic (M_1) and quasiantiferromagnetic (M_2) AFMR modes of frequencies $\nu_{1,2}$ (Fe), excited respectively at $\mathbf{h} \perp \mathbf{m}$ and $\mathbf{h} \parallel \mathbf{m}$, where \mathbf{m} is the weakly ferromagnetic moment. The two other lines, excited respectively by fields $\mathbf{h} \parallel \mathbf{a}$ and $\mathbf{h} \parallel \mathbf{b}$, are broader ($\Delta\nu/\nu \sim 1$) and are observed only at low temperatures ($T < 120$ K), when their intensities are high enough. In the Γ_2 phase at $T < 40$ K their frequencies are practically equal, while in transitions to the Γ_4 phase ($T > 60$ K) there is observed in the investigated frequency band only one mode in the $\mathbf{h} \parallel \mathbf{b}$ polarization, whose frequency decreases from 200 to 100

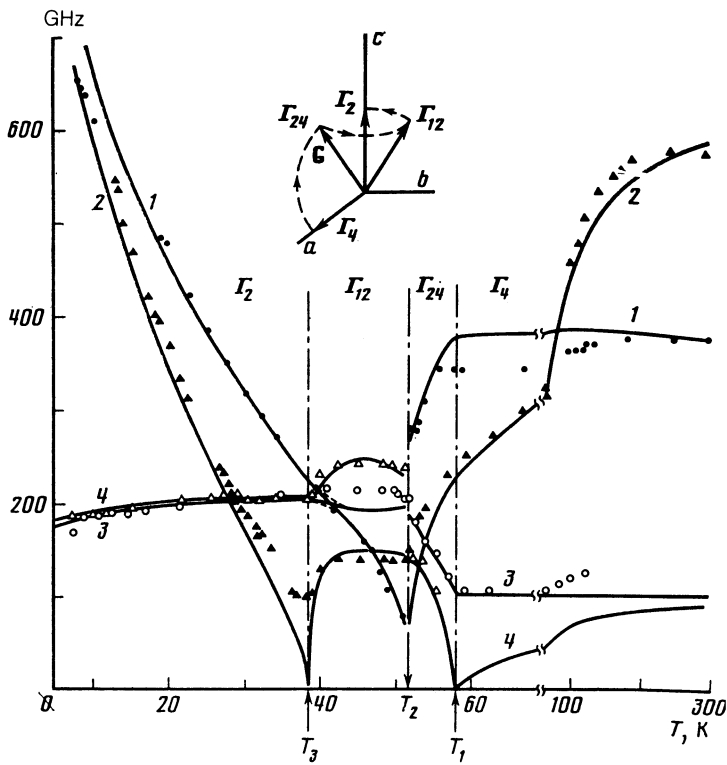


FIG. 1. Temperature dependences of the resonance frequencies: 1— $\nu_1(\text{Fe})$, 2— $\nu_2(\text{Fe})$, 3— $\nu_3(\text{R})$, 4— $\nu_4(\text{R})$. The inset shows the character of the rotation of the vector \mathbf{G} in the course of the spin reorientation $\Gamma_4-\Gamma_{24}-\Gamma_{12}-\Gamma_2$. The points in Figs. 1–3 are experimental, and the curves calculated.

GHz. Based on the frequencies, excitation conditions, and intensity temperature dependences of these absorption lines, we have identified them with the rare-earth modes ($\text{R}_{3,4}$) connected with electronic transitions between the energy levels of the ground quasidoublet of the Ho^{3+} ion. Their frequencies $\nu_{3,4}(\text{R}) \approx 200$ GHz in the Γ_2 phase correspond to Ho^{3+} doublet splitting obtained from the optical investigations ($2\Delta_{\text{R}} = 6-7.5 \text{ cm}^{-1}$),¹⁷⁻¹⁹ and the observed decrease of $\nu_3(\text{R})$ to 100 GHz on going to the Γ_4 phase, due to the vanishing of the exchange contribution Δ_{ex} , agrees well with the quasidoublet splitting in the crystal field ($2\Delta_{\text{R}} = 2\Delta_{\text{cf}} = 3.3 \text{ cm}^{-1}$).¹⁹

To determine the parameters of the observed modes, the $T(\nu)$ spectra were reduced for each T and polarization \mathbf{h} by the procedure of Ref. 10, using for the dispersion of the magnetic permeability $\mu_{\alpha}(\nu)$ the harmonic-oscillator model:

$$\mu_{\alpha}(\nu) = 1 + \sum_k \mu_{\alpha}^{(k)} \nu_k^2 / (\nu_k^2 - \nu^2 + i\Delta\nu_k \nu), \quad (1)$$

where ν_k and $\Delta\nu_k$ are the resonance frequency and the linewidth of the k th mode, and $\mu_{\alpha}^{(k)}$ is the contribution of this mode to the static magnetic permeability ($\alpha = x, y, z$). The results were the temperature dependences of the resonance frequencies ν_k , of the linewidths $\Delta\nu_k$, and of the contributions $\mu_{\alpha}^{(k)}$, which are shown in Figs. 1–3. A characteristic feature of the behavior of the resonance frequencies (Fig. 1) is the relaxation of both AFMR frequencies in the region $T = 35-65$ K, which attests to a decrease of the anisotropy energy, but in different planes of the crystal. At $T_1 = 58 \pm 2$ K, $T_2 = 51 \pm 1$ K, and $T_3 = 39 \pm 2$ K the temperature dependences of the resonance frequencies as well as of the linewidths (Fig. 2) and the mode contributions (Fig. 3) reveal anomalies that point to the existence of orientational phase transitions at these values of T .

We note first of all that the frequency relaxation of the

AFMR M_1 mode $\nu_1(\text{Fe})$, in which the vector \mathbf{G} oscillates in the ac plane, is evidence of the presence of reorientation of \mathbf{G} in this plane, realized apparently in the interval T_1-T_2 [canted phase $\Gamma_{24}(G_{z,x}, F_{x,z})$]. Attention is called to the asymmetric character of the behavior of $\nu_1(\text{Fe})$: its strong relaxation on the lower limit T_2 and the absence of relaxation on the upper limit T_1 . According to the classical model,²⁴ spin reorientation in the ac plane, which is effected via two sec-

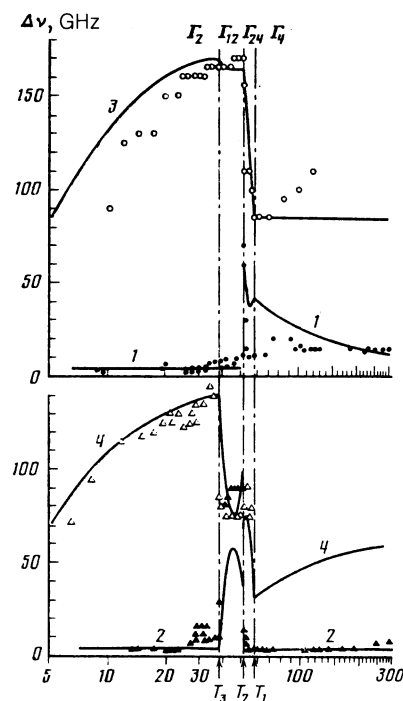


FIG. 2. Temperature dependences of the linewidths: 1— $\Delta\nu_1(\text{Fe})$, 2— $\Delta\nu_2(\text{Fe})$, 3— $\Delta\nu_3(\text{R})$, 4— $\Delta\nu_4(\text{R})$.

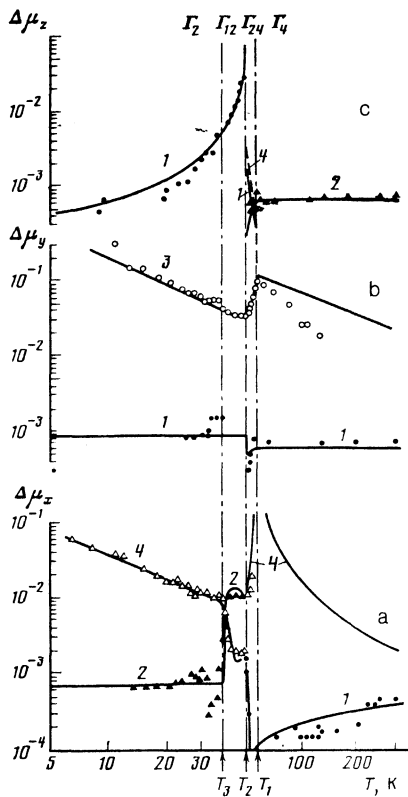


FIG. 3. Temperature dependences of the contributions of the modes to the static magnetic permeability: a) along the a (x) axis, where 1— $\Delta\mu_x^{(1)}$ (Fe), 2— $\Delta\mu_x^{(2)}$ (Fe), 4— $\Delta\mu_x^{(4)}$ (R); b) along the b (y) axis, where 1— $\Delta\mu_y^{(1)}$ (Fe), 3— $\Delta\mu_y^{(3)}$ (R); c) along the c (z) axis, where 1— $\Delta\mu_z^{(1)}$ (Fe), 2— $\Delta\mu_z^{(2)}$ (Fe), 4— $\Delta\mu_z^{(4)}$ (R).

ond-order PT ($\Gamma_4-\Gamma_{24}-\Gamma_2$), should be accompanied by relaxation of ν_1 at both reorientation limits. The reason why the observed behavior of ν_1 (Fe) in HoFeO₃ differs from the classical one is, as will be shown below, the interaction of this AFMR mode with a lower R mode.

We turn now to the anomalies observed at T_3 , which are of fundamental importance for the interpretation of the character of the spin reorientation in HoFeO₃. According to our data (Figs. 1–3) the following changes take place in the T_3 region: a) the M_2 -mode frequency ν_2 (Fe) passes through a minimum, while the R_4 -mode frequency ν_4 (R) rises above T_3 ; b) the linewidths and the contributions of the M_2 mode increase by more than an order, while those of the R_2 mode, on the contrary, decrease. The parameters of the remaining modes change little. Inasmuch as in the $\Gamma_2(G_z, F_x)$ phase the oscillations of the vector \mathbf{G} for the M_2 mode take place in the bc plane (symmetry of the Γ_{12} oscillations), the relaxation of its frequency ν_2 (Fe) at T_3 and other anomalies point to a transition, at the point T_3 , into the canted phase $\Gamma_{12}(G_{z,y}, F_x)$, in which the vector \mathbf{G} is deflected from the c axis in the bc plane. The small changes of the parameters of the M_1 and R_3 modes indicate that the angle of deflection of \mathbf{G} from the c axis in this phase is small ($\approx 10-20^\circ$). Notwithstanding the small deflection of \mathbf{G} from the c axis in the Γ_{12} phase, the interaction of the modes M_2 and R_4 increases compared with the Γ_2 phase (both modes are excited in the phases Γ_2 and Γ_{12} by a field $\mathbf{h}||\mathbf{a}$). As seen from Figs. 1–3, whereas in the Γ_2 phase the parameters of these modes change only weakly in the region of their crossing (≈ 30 K),

above T_3 , in the transition to the Γ_{12} phase, these modes become strongly hybridized, as manifested both by the increased separation of their frequencies and by the closer approach of their linewidths and contributions.

Judging from the behavior of the mode parameters, the canted phase Γ_{12} exists in the entire interval from T_3 to T_2 . The temperature T_2 (or a narrow region near it) is the boundary between the canted Γ_{12} and Γ_{24} . We have observed no indication of the existence of a bulk canted phase $\Gamma_{124}(G_{x,y,z})$ near T_2 . It can therefore be concluded on the basis of our experimental data that the spin reorientation is effected in HoFeO₃ in the form of three PT ($\Gamma_4-\Gamma_{24}-\Gamma_{12}-\Gamma_2$) rather than two ($\Gamma_4-\Gamma_{24}-\Gamma_2$) as heretofore assumed.^{1,20}

III. THEORY AND COMPARISON WITH EXPERIMENT

1. Spin-Hamiltonian of rare-earth subsystem

The central problem in the magnetism of orthoferrites is the description of the R subsystem with account taken of the real spectrum of the REI in a low-symmetry crystal field of C_s symmetry and for its exchange interaction with the Fe subsystem. In HoFeO₃ the ground state of the Ho³⁺ ion in the crystal field is a quasidoublet (two close singlets), separated from the excited states by an energy $\Delta E \approx 120$ K; the wave functions of the quasidoublet pertain to two different representations of the point group C_s .^{1,18} Thus, at $T < \Delta E$ the behavior of the R subsystem can be described in the two-level approximation on the basis of an effective Hamiltonian with spin $S_{\text{eff}} = 1/2$, which we write, following Ref. 25, in the form

$$\mathcal{H}_{\text{eff}} = - \sum_i [\Delta_{\text{cf}} \sigma_i^z + (\mu_0^i (\mathbf{H} + a\mathbf{F}) + B\mathbf{G}_z) \sigma_i^x] - \frac{1}{2} \sum_{i,j} \lambda_{ij} \sigma_i^x \sigma_j^x + \sum_i \Delta E_{\text{VV}}^i, \quad (2)$$

where \mathbf{F} and \mathbf{G} are the dimensionless ferromagnetism and antiferromagnetism vectors of the Fe subsystem, which we describe in the two-sublattice approximation, $\sigma = (\sigma_x^i, \sigma_y^i, \sigma_z^i)$ are Pauli matrices of the i th REI, $2\Delta_{\text{cf}}$ is the quasidoublet splitting in the crystal field, $\mu_0^i = \mu_0^\pm = (\mu_x, \pm \mu_y, 0)$ is the quasidoublet magnetic moment, \mathbf{H} is the external magnetic field, a and B are respectively the isotropic and anisotropic R–Fe exchange constants, and λ_{ij} are the R–R interaction constants. The “ \pm ” signs correspond to the two crystallographic nonequivalent positions of the REI. The quantities $\Delta E_{\text{VV}}^i = \Delta E_{\text{VV}}^i(\mathbf{H}, \mathbf{F}, \mathbf{G})$ represent the shift of the “center of gravity” of the REI quasidoublet on account of mixing of the excited states by the R–Fe interaction and by the external field. They are obtained in second-order perturbation theory in these interactions (the analog of the Van Vleck paramagnetism) and contribute to the susceptibility, the spontaneous magnetization, and the anisotropy energy of the system; this contribution will be taken into account phenomenologically below.

2. Equations of motion and thermodynamic potential of the nonequilibrium state

The R subsystem will be described with its nonequilibrium state defined by the mean values of the Pauli matrices $\langle \sigma^i \rangle$ of the i th ion, omitting henceforth the averaging sym-

bol ($\langle \sigma^i \rangle = \sigma^i$). The dynamic equations for σ^i , which can be obtained as in Ref. 26 by the nonequilibrium-statistical-operator method,^{27,28} are of the form

$$1/2\hbar\dot{\sigma}^i = -[\sigma^i\Phi_\sigma^i] + \mathbf{R}_i, \quad (3)$$

where $\Phi_\sigma^i = \partial\Phi/\partial\sigma^i$, $\Phi(\mathbf{F}, \mathbf{G}, \sigma^i)$ is the thermodynamic potential (TP) of the nonequilibrium state of the system, and \mathbf{R}_i are terms due to relaxation, which we shall describe phenomenologically (see, e.g., Ref. 29) by writing for \mathbf{R}_i the following simplest expansion in terms of Φ_i :

$$\mathbf{R}_i = -\lambda_0^0\Phi_\sigma^i - \lambda_{\perp}^0[(\sigma^i)^2\Phi_\sigma^i - \sigma^i(\sigma^i\Phi_\sigma^i)] - \lambda_{\parallel}^0\sigma^i(\sigma^i\Phi_\sigma^i), \quad (4)$$

where $\lambda_{0,\perp,\parallel}^0$ are the dissipation constants. Changing over to the approximation of two R-sublattices corresponding to two nonequivalent positions of the REI ($\sigma_1 = \sigma^i$ for i from the first sublattice and $\sigma_2 = \sigma^i$ for i from the second sublattice), and introducing the variables $\mathbf{f} = (\sigma_1 + \sigma_2)/2$ and $\mathbf{c} = (\sigma_1 - \sigma_2)/2$, we obtain for them from (3) the equations

$$(M_B/\gamma)\dot{\mathbf{f}} = -[\mathbf{f}\Phi_f] - [\mathbf{c}\Phi_c] + \mathbf{R}(\mathbf{f}, \mathbf{c}, \Phi_f, \Phi_c), \quad (5)$$

$$(M_B/\gamma)\dot{\mathbf{c}} = -[\mathbf{f}\Phi_c] - [\mathbf{c}\Phi_f] + \mathbf{R}(\mathbf{c}, \mathbf{f}, \Phi_c, \Phi_f),$$

where

$$\begin{aligned} \mathbf{R}(\mathbf{x}, \mathbf{y}, \Phi_x, \Phi_y) = & -\lambda_0\Phi_x - \lambda_{\perp}\{(x^2+y^2)\Phi_x + 2(xy)\Phi_y\} \\ & - (\lambda_{\perp} - \lambda_{\parallel})\{\mathbf{x}(\mathbf{x}\Phi_x) \\ & + \mathbf{x}(\mathbf{y}\Phi_y) + \mathbf{y}(\mathbf{x}\Phi_x) + \mathbf{y}(\mathbf{y}\Phi_y)\}, \end{aligned} \quad (6)$$

$$\Phi_x = \partial\Phi/\partial\mathbf{x}, \quad \Phi_y = \partial\Phi/\partial\mathbf{y}, \quad \lambda_{0,\perp,\parallel} = \lambda_{0,\perp,\parallel}^0/2N,$$

$\gamma = 2\mu_B/\hbar$, $M_B = \mu_B N$, μ_B is the Bohr magneton, and N is the number of ions per cm^3 .

We describe the dynamics of the Fe subsystem on the basis of the Landau-Lifshitz equations, which are similar to (5) when account is taken of the longitudinal relaxation:

$$(M_0/\gamma)\dot{\mathbf{F}} = [\mathbf{F}\Phi_F] + [\mathbf{G}\Phi_G] + \mathbf{R}'(\mathbf{F}, \mathbf{G}, \Phi_F, \Phi_G), \quad (7)$$

$$(M_0/\gamma)\dot{\mathbf{G}} = [\mathbf{F}\Phi_G] + [\mathbf{G}\Phi_F] + \mathbf{R}'(\mathbf{G}, \mathbf{F}, \Phi_G, \Phi_F),$$

where \mathbf{R}' is defined by (6) with $\lambda_{0,\perp,\parallel}$ replaced by the dissipation parameters $\Lambda_{0,\perp,\parallel}$ of the Fe subsystem; $M_0 = \mu_{\text{Fe}} N$, $\mu_{\text{Fe}} = 5\mu_B$.

We represent the nonequilibrium TP in the molecular-field approximation in the form²⁵

$$\begin{aligned} \Phi(\mathbf{F}, \mathbf{G}, \mathbf{f}, \mathbf{c}) = & \tilde{\Phi}_{\text{Fe}}(\mathbf{F}, \mathbf{G}) - N\{f_x[\mu_x(H_x + aF_x) + BG_x] \\ & + f_z\Delta_{\text{cf}} + c_x\mu_y(H_y + aF_y) \\ & + 1/2\lambda_f f_x^2 + 1/2\lambda_c c_x^2 + 1/2T[S(\sigma_1) + S(\sigma_2)]\}, \end{aligned} \quad (8)$$

where

$$S(\sigma) = \ln 2^{-1/2}(1+\sigma)\ln(1+\sigma) - 1/2(1-\sigma)\ln(1-\sigma),$$

$$\sigma_{1,2} = |\mathbf{f} \pm \mathbf{c}|,$$

λ_f and λ_c are the R-R interaction constants,

$$\begin{aligned} \tilde{\Phi}_{\text{Fe}} = & \Phi_{\text{Fe}} + \sum_i \Delta E_{\text{VV}}^i = 1/2AF^2 + 1/2D(\mathbf{F}\mathbf{G})^2 - d(F_xG_x - F_zG_z) \\ & - M_0\mathbf{F}\mathbf{H} - \tau_1^{\text{VV}}H_xG_x - \tau_3^{\text{VV}}H_zG_x - 1/2\sum_{\alpha} \chi_{\alpha}^{\text{VV}}H_{\alpha}^2 + \Phi_A(\mathbf{G}), \end{aligned} \quad (9)$$

$$\begin{aligned} \Phi_A(\mathbf{G}) = & 1/2K_{ac}^0G_z^2 + 1/2K_{ab}^0G_y^2 + 1/4K_2G_z^4 \\ & + 1/4K_2'G_y^4 + 1/2K_2''G_z^2G_y^2, \end{aligned} \quad (10)$$

and $\tilde{\Phi}_{\text{Fe}}$ is the TP of the Fe subsystem, renormalized by the Van Vleck corrections to the quasidoublet energy. The most important for us is renormalization of the anisotropy constants ($K_{ac}^0 = K_{ac}^{\text{Fe}} + K_{ac}^{\text{VV}}$, $K_{ab}^0 = K_{ab}^{\text{Fe}} + K_{ab}^{\text{VV}}$).

3. Static magnetic properties. Spin-reorientation mechanism

We calculate the equilibrium values of the order parameters in the phases $\Gamma_2, \Gamma_4, \Gamma_{12}$ and Γ_{24} and analyze their stability. Minimizing (8) with respect to \mathbf{F}, \mathbf{f} , and \mathbf{c} under the conditions $G^2 = 1 - F^2 = 1$ and $\mathbf{F}\cdot\mathbf{G} = 0$ (since the temperatures are low enough and the Fe sublattices are saturated ($D \rightarrow \infty$)), we find for the phases Γ_2, Γ_{24} , and Γ_4 that $f_y = F_y = \mathbf{c} = 0$,

$$\begin{aligned} f_x = f_0 \sin \psi = & \Delta_{\text{cx}}^0 G_z / (T - \tilde{\lambda}_f), \quad f_z = f_0 \cos \psi, \\ F_x = F_0 G_z, \quad F_z = & -F_0 G_x, \end{aligned} \quad (11)$$

where

$$\begin{aligned} F_0 = (d + Na\mu_x f_x G_z) / A, \quad \tilde{T} = & \Delta_R / \text{th}(\Delta_R/T), \quad f_0 = \text{th}(\Delta_R/T), \\ \sin \psi = \Delta_{\text{cx}} / \Delta_R, \quad \cos \psi = & \Delta_{\text{cz}} / \Delta_R, \quad \Delta_R^2 = \Delta_{\text{cz}}^2 + \Delta_{\text{cx}}^2. \end{aligned} \quad (12)$$

In the phase Γ_{12} the order parameters are determined also by expressions (11) and (12), except that

$$G_x = F_z = 0, \quad F_x = (dG_z + Na\mu_x f_x) / A, \quad \tilde{\lambda}_f = \lambda_f + \Delta\lambda_f.$$

Substituting (11) in (8) we obtain a TP that depends only on \mathbf{G} . In collinear phases we have $G_x = \pm 1, G_z = 0$ (Γ_4) and $G_x = 0, G_z = \pm 1$ (Γ_2). The stability of these phases is determined from the conditions that the increment of $\Phi(\mathbf{G})$ be positive-definite when \mathbf{G} deviates from the equilibrium values:

$$\Delta\Phi_{\Gamma_4} = 1/2K_{ac}\Delta G_z^2 + 1/2K_{ab}\Delta G_y^2, \quad \Delta\Phi_{\Gamma_2} = 1/2K_{ca}\Delta G_x^2 + 1/2K_{cb}\Delta G_y^2, \quad (13)$$

where

$$\begin{aligned} K_{ac} = K_{ac}^0 - N(\Delta_{\text{cx}}^0)^2 / (T - \tilde{\lambda}_f), \quad K_{ab} = & K_{ab}^0 + d^2/A = \tilde{K}_{ab}^{\text{Fe}} + K_{ab}^{\text{VV}}, \\ K_{ca} = N(\Delta_{\text{cx}}^0)^2 (1 + \varepsilon) / (T - \tilde{\lambda}_f) - & K_{ac}^0 - K_2, \quad (14) \\ K_{cb} = K_{ab} + K_2'' - K_{ac}^0 - K_2 + N(\Delta_{\text{cx}}^0)^2 / & (T - \tilde{\lambda}_f), \\ \varepsilon = \Delta\lambda_f / (T - \tilde{\lambda}_f), \quad \Delta\tilde{\lambda}_f = \lambda_f + \Delta\lambda_f, \quad & \tilde{K}_{ab}^{\text{Fe}} = K_{ab}^{\text{Fe}} + d^2/A. \end{aligned}$$

The quantities $K_{ac}, K_{ab}, K_{ca}, K_{cb}$ determine the AFMR frequencies and characterize the rigidity of the system when \mathbf{G} deviates from equilibrium, provided that \mathbf{F}, \mathbf{f} , and \mathbf{c} follow \mathbf{G} in equilibrium fashion. For $T \gg \Delta_R$, where $\tilde{T} \rightarrow T$, they go over into the usual effective anisotropy constants in the corresponding planes. The TP of the system can be represented in this case in the form (10) $\Phi(\mathbf{G}) = \Phi_A(\mathbf{G})$, in which we must substitute $K_{ac,ab}^0 \rightarrow \tilde{K}_{ac,ab}$, $K_2 \rightarrow K_{2\text{eff}}$, and $K_2'' \rightarrow K_{2\text{eff}}''$, where $K_{ac,ab}$ is defined in (14) and

$$K_{2\text{eff}} = K_2 - 2\Delta K, \quad K_{2\text{eff}}'' = K_2'' - \Delta K,$$

$$\Delta K = \Delta\lambda_f (\Delta_{\text{cx}}^0)^2 / (T - \lambda_f)^2.$$

The stability of the phases and the character of phase transition for spin reorientation can be illustratively tracked on a phase diagram in the space of the anisotropy constants K_{ac} and K_{ab} (Fig. 4) obtained by minimizing $\Phi(\mathbf{G})$. We have assumed here that $\tilde{K}_{2\text{eff}} = K_{2\text{eff}} + K_2' - 2K_{2\text{eff}}'' > 0$, as follows from the condition that the canted phases Γ_{24} and Γ_{12} exist and that $K_2' < 0$ according to the data of Refs. 1 and 10 for DyFeO_3 . In this case the stability-loss lines of the

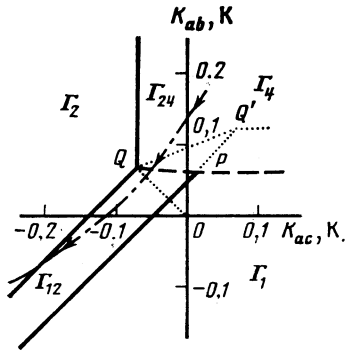


FIG. 4. Phase diagram of orthoferrite in the space of the second-order anisotropy constants K_{ac} and K_{ab} (numerical calculation for HoFeO_3); the solid lines correspond to a second order PT, the dashed to a first-order PT, and the dotted to stability-loss lines. The point coordinates are: $Q(-K_{2\text{eff}}, -K'_{2\text{eff}})$, $M(-K'_{2\text{eff}}, -K'_2)$, $P(\frac{1}{2}K'_2 - K'_{2\text{eff}}, -\frac{1}{2}K'_2)$.

phases Γ_4 ($K_{ac}(T_1) = 0$) and $\Gamma_2(K_{cb} \times (T_3) = K_{ab} - K_{ac} - K_{2\text{eff}} + K'_{2\text{eff}} = 0)$ are lines of the second-order phase transitions $\Gamma_4 - \Gamma_{24}$ and $\Gamma_{12} - \Gamma_2$, respectively, while the regions of the existence of the phases Γ_{12} and Γ_{24} overlap and a first-order phase transition takes place between them. The angles that determine the orientation of \mathbf{G} on the planes ac (Γ_{24}) and bc (Γ_{12}) are given by $\cos^2\theta_1 = K_{ac}/K_{2\text{eff}}$ and $\sin^2\theta_2 = -k_{cb}/\tilde{K}_{2\text{eff}}$. Note that for $K_{2\text{eff}}, K'_2 > 0$ and $K_{2\text{eff}}K'_2 > (K_{2\text{eff}})^2$ the reorientation from the phase Γ_{24} into Γ_{12} is a smooth one via the bulk canted phase $\Gamma_{124}(G_{x,y,z})$ (see also Ref. 30). In the case of HoFeO_3 , however, we favor first variant, which corresponds to the more realistic condition $K'_2 < 0$ and, as shown by calculations, agrees better with experiment.

It can thus be concluded that spin reorientation in HoFeO_3 proceeds in the form of three PT ($\Gamma_4 - \Gamma_{24} - \Gamma_{12} - \Gamma_2$), in the course of which the vector \mathbf{G} is deflected from the a axis (Γ_4) at the upper boundary T_1 and rotates smoothly in the ac plane (Γ_{24}) and then, without reaching the c axis ($10-20^\circ$) it is jumpwise reoriented at T_2 into the bc plane (Γ_{12}) in which it already rotates smoothly to the c axis at T_3 (Γ_2).

As follows from Fig. 4, a feature of the spin reorientation in HoFeO_3 is that the thermodynamic path of the system on the $K_{ab} - K_{ac}$ plane passes near the origin, where both anisotropy constants K_{ac} and K_{ab} reverse sign. The mechanism of the $K_{ac}(T)$ temperature dependence is determined mainly by the Zeeman contribution due to the anisotropy of the exchange splitting of the ground quasidoublet of the Ho^{3+} doublet [see (14)]. As for $K_{ab}(T)$, according to (14), there is no such contribution here. Therefore the observed decrease of K_{ab} when T is lowered can be naturally attributed to the temperature dependence of the Van Vleck contribution $K_{ab}^{\text{VV}}(T)$ due to the change of the population of the excited Ho^{3+} levels (as, e.g., in DyFeO_3 , Ref. 1). We express the displacements of the gravity centers of the ground ($i = 1$) and excited ($i \geq 2$) quasidoublets as

$$\Delta E_{\text{VV}}^{(i)} = \text{const} + \Delta E_{ac}^{(i)} G_z^2 + \Delta E_{ab}^{(i)} G_y^2,$$

where $\Delta E_{ac,ab}^{(i)}$ are phenomenological constants. In this case we have, by analogy with Ref. 25, for the $K_{ab,ac}(T)$ dependence

$$K_{ab,ac}^{\text{VV}}(T) = 2 \sum_i \Delta E_{ab,ac}^{(i)} \exp\left(-\frac{E_i^0}{T}\right) / \sum_i \exp\left(-\frac{E_i^0}{T}\right),$$

where E_i^0 is the energy of the gravity centers of the unperturbed quasidoublets of the Ho^{3+} ion in the crystal field: $E_1^0 = 0, E_2^0 = 120$ K (Ref. 17), and numerical calculations show that it suffices to take the remaining levels into account by introducing their gravity center $E_s^0 \approx 300$ K.

4. Dynamic properties of rare-earth subsystem

Let us calculate the high-frequency magnetic susceptibility of the R subsystem relative to the external field \mathbf{h} , assuming \mathbf{F} and \mathbf{G} to be equal to their static values. Linearizing the equations of motion (5), which break up into two groups corresponding to the Δf oscillations excited by the field $\mathbf{h} \parallel \mathbf{a}$ and to the Δc oscillations excited by the field $\mathbf{h} \parallel \mathbf{b}$, and omitting the inessential $\chi_{\alpha}^{\text{VV}}$, we get

$$\chi_x^{\text{R}}(p) = (Nf_0\mu_x^2/\mu_B) [\Delta_{\perp}'(p)(p + \omega_r') \cos^2 \psi + \delta_{\parallel} \Delta_{\perp}(p) \sin^2 \psi] / \Delta(p), \quad (15)$$

where

$$\begin{aligned} p &= i\omega, \quad \Delta(p) = (p + \omega_r) \Delta_{\perp}(p) - \delta_{\parallel} \omega_r^2 \Delta_{\perp}'(p) \sin^2 2\psi, \\ \Delta_{\perp}(p) &= p^2 + \omega_R \omega_r' (1 + \delta_{\perp}^2) + p \Delta \omega_R, \\ \Delta_{\perp}'(p) &= \omega_R (1 + \delta_{\perp}^2) + \delta_{\perp} p, \\ \omega_i &= -\lambda_i f_0 / \hbar, \quad \omega_R = 2\Delta_R / \hbar, \quad \omega_r' = \omega_r + 2\omega_f \cos^2 \psi, \\ \omega_r &= \omega_r^0 + \delta_{\parallel} \omega_f \sin^2 \psi, \quad \omega_r' = \omega_r^0 - \delta_{\parallel} \omega_f \sin^2 \psi, \\ \omega_r^0 &= 2\delta_{\parallel} T f_0 / \hbar (1 - f_0^2), \quad \Delta \omega_R = \delta_{\perp} (\omega_R + \omega_r'), \\ \delta_{\perp, \parallel} &= (\lambda_0 + \lambda_{\perp, \parallel} f_0^2) / f_0. \end{aligned} \quad (16)$$

The quantities Δ_R , ψ , and f_0 are defined in (11) and (12). The susceptibility along the y axis (b axis) is also defined by expressions (15) and (16) in which we must substitute $\mu_x \rightarrow \mu_y$ and $\lambda_f \rightarrow \lambda_c$. Expression (15) describes the susceptibility frequency dependence due to the REI effective-spin longitudinal and transverse oscillations that interact with one another. For weak interaction ($|\lambda_{f,c}| \ll T$) their frequencies are characterized respectively by the longitudinal-relaxation frequency ω_r and by the resonance (complex) frequency

$$\omega_{\text{R}\pm} = \pm [\omega_R \omega_r' (1 + \delta_{\perp}^2) - \Delta \omega_R^2 / 4]^{1/2} + i \Delta \omega_R / 2,$$

which is determined by the electronic transitions between the energy levels of the quasidoublet, and represents in fact the paramagnetic-resonance frequency. At low frequencies ($\omega \sim \omega_r \ll |\omega_R|$)

$$\chi_x^{\text{R}}(p) = (\chi_x^{\text{R}})_{\perp} + (\chi_x^{\text{R}})_{\parallel} \bar{\omega}_r / (\bar{\omega}_r + p), \quad (17)$$

where

$$\begin{aligned} (\chi_x^{\text{R}})_{\perp} &= \chi_{x_0}^{\text{R}} \cos^2 \psi, \quad (\chi_x^{\text{R}})_{\parallel} = \chi_{x_0}^{\text{R}} (\delta_{\parallel} \omega_R^2 / \omega_r' \bar{\omega}_r) \sin^2 \psi, \\ \chi_{x_0}^{\text{R}} &= N f_0 \gamma \mu_x^2 / \mu_B \omega_r', \quad \bar{\omega}_r = \omega_r^0 + \delta_{\parallel} \omega_f (\omega_r / \omega_r') \sin^2 \psi, \end{aligned} \quad (18)$$

$(\chi_x^{\text{R}})_{\perp, \parallel}$ are the contributions of the transverse and longitudinal oscillations to the static susceptibility with which $\chi_x^{\text{R}}(p)$ coincides in the limit as $p \rightarrow 0$:

$$\begin{aligned} (\chi_x^{\text{R}})_{\text{st}} &= \chi_x^{\text{R}}(0) = (\chi_x^{\text{R}})_{\perp} + (\chi_x^{\text{R}})_{\parallel} \\ &= N \mu_x^2 \left[\frac{T \Delta_R}{T f_0 \cos^2 \psi + \Delta_R (1 - f_0^2) \sin^2 \psi} - \lambda_f \right]^{-1}. \end{aligned} \quad (19)$$

For $\omega \sim \omega_R \gg \omega_r$, we have when the longitudinal oscillations

tions are "frozen"

$$\chi_x^R(p) = (\chi_x^R)_\perp \omega_R' \Delta_\perp'(p) / \Delta_\perp(p). \quad (20)$$

Let us analyze on the basis of (15)–(20) the observed high-frequency properties of the R subsystem in HoFeO₃. We use as an example the R₃ mode excited by a field $\mathbf{h} \parallel \mathbf{b}$ and interacting weakly with the AFMR modes. We note first that the frequency of this mode (Fig. 1), which is proportional to the splitting $2\Delta_R$ of the ground quasidoublet of Ho³⁺, follows well the variation of the latter in the course of the spin reorientation. The increase of $\nu_3(\mathbf{R})$ on going from the phase Γ_4 to the phases Γ_{24} , Γ_{12} , and Γ_2 is due to the growth of the exchange splitting, $\Delta_{ex} \propto G_z$. The small decrease of $\nu_3(\mathbf{R})$ with decrease of T is due to the antiferromagnetic character of the R–R interaction ($\lambda_{fc} < 0$), which decreases Δ_R somewhat (see also Ref. 17).

Consider the behavior of the contribution $\Delta\mu_y^{(3)}(\mathbf{R}) = 4\pi(\chi_y^R)_\perp$ of this mode (Fig. 3b). Its increase ($\propto 1/T$) when T is lowered is due to the decrease of the Ho³⁺ quasidoublet upper-level population, as a result of which the total static susceptibility $(\chi_y^R)_{st}$ also increases. The $\Delta\mu_y^{(3)}(\mathbf{R})$ anomaly observed in the spin-reorientation region is due to the strong dependence of the contributions of the considered resonance R-mode on the angle $\psi = \tan^{-1}(\Delta_{ex}/\Delta_{cf})$, and also of the low-lying relaxation R mode. According to (18), on going from the Γ_4 phase where $\Delta_{ex} = 0$ and $\cos \psi = 1$ to the phases Γ_{24} , Γ_{12} , and Γ_2 , where $\Delta_{ex} \neq 0$ and $\cos \psi < 1$, the contribution $\Delta\mu_y^{(3)}(\mathbf{R})$ of the resonance R-mode should decrease, as is indeed observed in experiment. It follows also directly that in the phase Γ_2 , Γ_{24} , and Γ_{12} , where $(\chi_y^R)_\perp < (\chi_y^R)_{st}$, there exists a low-lying re-

laxational R-mode excited by a field $\mathbf{h} \parallel \mathbf{b}$ and "frozen" in the frequency range investigated by us. In the Γ_4 phase this mode also exists, but cannot be excited by an external magnetic field.

We turn now to the behavior of the linewidths $\Delta\nu_{3,4}(\mathbf{R})$ of the observed resonance R modes. In the Γ_2 phase, at low T , they increase rapidly as t is raised and subsequently saturate to 160 and 130 GHz for the modes R₃ and R₄, respectively. The most probable causes of so large an R-mode width are, in our opinion, the dipole and exchange R–R interactions, since the scatter (fluctuations) of the local effective fields ($\Delta H \approx 1\text{--}5$ kOe) which they produce at the REI in a concentrated system is of the same order of the observed linewidths of these modes. The temperature dependence of the linewidths in the Γ_2 phase can be explained on the basis of the moment theory used in EPR to analyze line shapes in spin–spin interactions. According to Ref. 31, the temperature dependence of the second moment that determines the square of the linewidth is of the form $M_2 \sim 1 - f_0^2(T)$, in good agreement with the observed behavior of $\Delta\nu_{3,4}(\mathbf{R})$ in the Γ_2 phase.

An important feature of the behavior of the linewidth $\Delta\nu_3(\mathbf{R})$ is its noticeable decrease as \mathbf{G} becomes reoriented from the c to the a axis in the interval $T_2 < T < T_1$ (Fig. 3a). Since this is accompanied by a decrease of the quantity $\Delta_{ex} \propto G_z$ that determines the effective field $\mathbf{h}_{eff} = (\Delta_{cf}, 0, \Delta_{ex})$ acting on the effective spin of the Ho³⁺ quasidoublet, we can conclude that the relaxation rate in the R subsystem depends on \mathbf{h}_{eff} or, in this case, on G_z . In the context of our phenomenological description of the relaxation, this can be taken into account by introducing the dependences of the

TABLE I. Parameters of magnetic interactions in HoFeO₃ and YFeO₃ (per formula unit)

Parameters	HoFeO ₃		YFeO ₃	
	Present paper	[19]	[33]	[34]
Δ_{cf}, K	2.4	2.3±0.2	–	–
Δ_{ex}^0, K	4.7	4.8±0.3	–	–
μ_x, μ_B	3.25	3.6±0.1	–	–
μ_y, μ_B	7.2	7.9±0.5	–	–
λ_f, K	–3.5	–	–	–
λ_c, K	–2.5	–	–	–
$K_{ac}^0 = K_{ac}^{Fe} + 2\Delta E_{ac}^{(1)}, \text{K}$	0.30	–	0.23	0.29
$\Delta E_{ac}^{(2)}, \text{K}$	0.36	–	0	0
$\Delta E_{ac}^{(3)}, \text{K}$	0.3	–	0	0
$K_2 = K_2^{Fe}, \text{K}$	0.07	–	0.175	–
$K_{ab}^0 = K_{ab}^{Fe} + 2\Delta E_{ab}^{(1)}, \text{K}$	–0.173	–	–	1.14
$\Delta E_{ab}^{(2)}, \text{K}$	1.35	–	0	0
$\Delta E_{ab}^{(3)}, \text{K}$	0.6	–	0	0
K_2', K	–0.12	–	–	–
K_2'', K	–0.07	–	–	–
H_B, Oe	8·10 ⁶	–	–	6.4·10 ⁶
H_D, Oe	1.2·10 ⁵	–	–	1.4·10 ⁵
a, Oe	–0.8·10 ⁵	–	0	0
m_x^0, μ_B	0.039	–	–	–
m_2^0, μ_B	0.07	–	0.059	–

corresponding dissipation constants in (4) and (6), and hence also of the R-mode linewidths, on G_z , viz., $\Delta\nu_R = \Delta\nu_{R_0}(1 + kG_z^2 + \dots)$, where ν_{R_0} and k are in the general case functions of T . For $\nu_{R_0}(T)$ with allowance for the foregoing, we can use a dependence in the form $\Delta\nu_{R_0}(T) = \Delta\nu_{R_0}^0 [1 - f_0^2(T)]^{1/2}$. A satisfactory quantitative description of the R-mode linewidths (Fig. 2) is obtained for $k = 0.9$ and $\nu_{R_0}^0 = 73$ GHz for $\Delta\nu_4(\mathbf{R})$ and $\nu_{R_0}^0 = 90$ GHz for $\Delta\nu_3(\mathbf{R})$ and the remaining parameters of the table. The frequencies and R-mode contributions calculated for the same parameters also agree well with experiment (Figs. 1 and 3). It can be seen that the behavior of the R_4 mode in the Γ_2 phase does not differ qualitatively from the considered R_3 mode, but in the phases Γ_{12} , Γ_{24} , and Γ_4 it turns out to be substantially different because of the interaction with the AFMR modes.

5. Dynamics of interacting Fe and R subsystems

Analysis of the equations of motion (5) and (7) shows the presence in the system of four resonance frequencies, two ($M_{1,2}$) corresponding to the AFMR modes of the Fe subsystem, with frequencies $\omega_{1,2}$ (Fe), and two resonance rare-earth modes ($R_{3,4}$) with frequencies $\omega_{3,4}$ (R). Note that even when the modes $M_{1,2}$ and $R_{3,4}$ are coupled, their parameters (linewidths, contributions) differ strongly as a rule, so that this distinction between the modes is justified. Besides the resonance mode there are also relaxation modes due to longitudinal oscillations of the alternating Fe and R subsystems. In our case, however, as shown by an analysis of the R subsystem, longitudinal oscillations having frequencies on the order of the resonance ones can be treated as frozen by subjecting the dynamic variables to the constraints

$$\begin{aligned} \Delta F G_0 + \Delta G F_0 = 0, \quad \Delta F F_0 + \Delta G G_0 = 0, \\ \Delta f c_0 + \Delta c f_0 = 0, \quad \Delta f f_0 + \Delta c c_0 = 0, \end{aligned}$$

where F_0 , G_0 , f_0 , and c_0 are the equilibrium values of the order parameters.¹ In this case, eight out of the 12 equations of motion are independent. In the canted phase Γ_{24} all the equations are coupled, while in the collinear phases Γ_4 and Γ_2 and in the canted Γ_{12} they break up into two groups corresponding to modes of different symmetry, which we characterize, in analogy with Ref. 6, by representations of the crystal group D_{2h}^{16} .

In the Γ_2 and Γ_{12} phases there are two modes of symmetry Γ_{12} (ΔF_x , $\Delta G_{y,z}$, $\Delta f_{\xi,\eta,\zeta}$), representing M_1 and R_4 modes, and also modes of symmetry Γ_{34} ($\Delta F_{x,y}$, ΔG_x , $\Delta c_{\xi,\eta,\zeta}$), which represent also interacting M_2 and R_3 modes. The complex frequencies of these modes are given by

$$p^4 + A_3 p^3 + A_2 p^2 + A_1 p + A_0 = 0, \quad (21)$$

where

$$\begin{aligned} p = i\omega, \quad A_0 = \omega_{10}^2 \omega_{20}^2 - \omega_{12}^4, \quad A_1 = \Delta\omega_{10} \omega_{20}^2 + \Delta\omega_{20} \omega_{10}^2 - \Delta\omega_{12}^3, \\ A_2 = \omega_{10}^2 + \omega_{20}^2 + \Delta\omega_{10} \Delta\omega_{20} - \Delta\omega_{12}^2, \quad A_3 = \Delta\omega_{10} + \Delta\omega_{20}. \end{aligned} \quad (22)$$

The quantities $\omega_{10,20}$ and $\Delta\omega_{10,20}$ are respectively the frequencies and linewidths of the Fe- and R-subsystem modes if they do not interact dynamically, while ω_{12} , $\Delta\omega_{12}$, and $\Delta\omega'_{12}$ determine the latter interaction. Depending on the magnetic phase and on the oscillation symmetry, they take on the following values:

Γ_2 phase. M_2 and R_4 of Γ_{12} symmetry:

$$\begin{aligned} \omega_{10}^2 = \omega_E \omega_{cb} (1 + \Lambda_{\perp}^2), \quad \omega_{20}^2 = \omega_R \omega_R' (1 + \delta_{\perp}^2), \\ \Delta\omega_{10} = \Lambda_{\perp}' (\omega_E + \omega_{cb}), \quad \Delta\omega_{20} = \delta_{\perp} (\omega_R + \omega_R'), \\ \omega_{12}^4 = \omega_R \omega_{cb} \omega_{ax} \omega_{ax}' (1 + \Lambda_{\perp}^2) (1 + \delta_{\perp}^2), \end{aligned} \quad (23)$$

$$\begin{aligned} \Delta\omega_{12}^3 = \omega_{ax} \omega_{ax}' [\delta_{\perp} (1 + \Lambda_{\perp}^2) \omega_{cb} + \Lambda_{\perp}' (1 + \delta_{\perp}^2) \omega_R], \\ \Delta\omega_{12}^2 = \Lambda_{\perp}' \delta_{\perp} \omega_{ax} \omega_{ax}', \quad \Lambda_{\perp}' = \Lambda_{\perp} + \Lambda_0, \quad \omega_E = \gamma A / M_0 = 2\gamma H_E, \\ \omega_{cb} = \gamma K_{cb} / M_0, \quad \omega_{ax} = \gamma a \mu_x \cos \psi / \mu_{Fe}, \quad \omega_{ax}' = \gamma a \mu_x f_i / \mu_B. \end{aligned}$$

For modes M_1 and R_3 of symmetry Γ_{34} the corresponding values are determined by (21)–(23) with the substitutions

$$\begin{aligned} \omega_{cb} \rightarrow \omega_{ca} = \gamma K_{ca} / M_0, \quad \omega_R' \rightarrow \omega_R'' = \omega_R - 2\lambda c f_0 \cos^2 \psi / \hbar, \\ \omega_{ax} \rightarrow \omega_{ay}, \quad \omega_{ax}' \rightarrow \omega_{ay}', \end{aligned}$$

where ω_{ay} and ω_{ay}' differ from ω_{ax} and ω_{ax}' in that μ_x is replaced by μ_y .

Γ_{12} phase. M_2 and R_4 modes of symmetry Γ_{12} :

$$\begin{aligned} \omega_{10}^2 = \omega_E \omega_{bc}^0 (1 + \Lambda_{\perp}^2), \quad \omega_{20}^2 = \omega_R \omega_R' (1 + \delta_{\perp}^2), \\ \Delta\omega_{10} = \Lambda_{\perp}' (\omega_E + \omega_{bc}^0), \quad \Delta\omega_{20} = \delta_{\perp} (\omega_R + \omega_R'), \\ \omega_{12}^4 = \omega_E \omega_R G_y^2 (\omega_{ex} \omega_{ex}' + \omega_{bc}^0 \omega_{ax} \omega_{ax}' / \omega_E) (1 + \delta_{\perp}^2) (1 + \Lambda_{\perp}^2), \\ \Delta\omega_{12}^3 \approx \omega_{ex} \omega_{ex}' G_y^2 [\delta_{\perp} (1 + \Lambda_{\perp}^2) \omega_E + \Lambda_{\perp}' (1 + \delta_{\perp}^2) \omega_R], \\ \Delta\omega_{12}^2 \approx \Lambda_{\perp}' \delta_{\perp} G_y^2 \omega_{ex} \omega_{ex}', \quad \omega_{ex} = \gamma \Delta_{ex}^0 \cos \psi / \mu_{Fe}, \\ \omega_{ex}' = \gamma \Delta_{ex}^0 f_i / \mu_B, \\ \omega_{bc}^0 = \gamma (K_{ac}^0 - K_{ab} + K_2'' - K_2' + 3K_2 G_z^2) G_y^2 / M_0. \end{aligned} \quad (24)$$

Modes M_1 and R_3 of symmetry Γ_{34} :

$$\begin{aligned} \omega_{10}^2 = \omega_E \omega_{ba} (1 + \Lambda_{\perp}^2), \quad \omega_{20}^2 = \omega_R \omega_R'' (1 + \delta_{\perp}^2), \\ \Delta\omega_{10} = \Lambda_{\perp}' (\omega_E + \omega_{ba}), \quad \Delta\omega_{20} = \delta_{\perp} (\omega_R + \omega_R''), \\ \omega_{12}^4 = \omega_R \bar{\omega}_{ba} \omega_{ay} \omega_{ay}' (1 + \Lambda_{\perp}^2) (1 + \delta_{\perp}^2), \quad \Delta\omega_{12}^3 \approx \delta_{\perp} \omega_{ay} \omega_{ay}' \bar{\omega}_{ba}, \\ \Delta\omega_{12}^2 \approx \delta_{\perp} \Lambda_{\perp}' \omega_{ay} \omega_{ay}', \quad \bar{\omega}_{ba} = \omega_{ba} G_z^2 + \omega_{ax}^0 f_i^2 G_y^2 / \omega_E, \\ \omega_{ba} = \gamma (-K_{ab} - K_2' G_y^2 - K_2'' G_z^2) / M_0 + \omega_{ax}^0 f_i^2 / \omega_E, \\ \omega_{ax}^0 = \gamma a \mu_x / \mu_{Fe}. \end{aligned} \quad (25)$$

In the Γ_{24} phase all four modes are generally speaking interacting (the oscillation symmetry correspond to the Γ_{1234} representation). They differ, however, in the degree of interaction. The strongest interaction is that of the modes M_1 and R_4 ; it is determined principally by an anisotropic R-Fe interaction exchange-enhanced on account of ω_E ($\omega_{12}^4 \sim \omega_E \omega_R \omega_{ex} \omega_{ex}'$) and exceeds substantially their interaction with the M_2 and R_3 modes and the interaction of the latter with one another. Taking this into account and neglecting the interaction of M_2 and R_3 with M_1 and R_4 , we can determine the frequencies of the latter from an equation of type (24) with parameters

$$\begin{aligned} \omega_{10}^2 = \omega_E \bar{\omega}_{ac}^0 (1 + \Lambda_{\perp}^2), \quad \omega_{20}^2 = \omega_R \omega_R' (1 + \delta_{\perp}^2), \\ \Delta\omega_{10} = \Lambda_{\perp}' (\omega_E + \bar{\omega}_{ac}^0), \quad \Delta\omega_{20} = \delta_{\perp} (\omega_R + \omega_R'), \\ \Delta\omega_{12}^4 = \omega_E \omega_R \omega_{ex} \omega_{ex}' G_x^2 (1 + \delta_{\perp}^2) (1 + \Lambda_{\perp}^2), \\ \Delta\omega_{12}^3 = \omega_{ex} \omega_{ex}' G_x^2 [\delta_{\perp} (1 + \Lambda_{\perp}^2) \omega_E + \Lambda_{\perp}' (1 + \delta_{\perp}^2) \omega_R], \\ \Delta\omega_{12}^2 = \Lambda_{\perp}' \delta_{\perp} \omega_{ex} \omega_{ex}' G_x^2, \quad \bar{\omega}_{ac}^0 = \gamma (K_{ac}^0 + 3K_2 G_E^2) G_x^2 / M_0. \end{aligned} \quad (26)$$

The frequencies of the M_2 and R_3 modes, neglecting their interaction, determined for the M_2 mode by the equation

$$\omega^2 - i\Delta\omega\omega - \omega_0^2 = 0,$$

where

$$\begin{aligned} \omega_0^2 = \omega_E \bar{\omega}_{ab} (1 + \Lambda_{\perp}^2), \quad \Delta\omega = \Lambda_{\perp}' (\omega_E + \bar{\omega}_{ab}), \\ \bar{\omega}_{ab} = \gamma (K_{ab} + K_2'' G_z^2) / M_0, \end{aligned}$$

and for the mode R_3 by

$$\omega_0^2 = \omega_R \omega_R'' (1 + \delta_{\perp}^2), \quad \Delta \omega = \delta_{\perp} (\omega_R + \omega_R'').$$

In the Γ_4 phase there is for the oscillations of symmetry Γ_{14} ($\Delta F_z, \Delta G_{x,y}$) only one AFMR mode M_2 , and for the oscillations of symmetry Γ_{23} ($\Delta F_{x,y}, \Delta G_z, \Delta f_{\xi,\eta}, \Delta c_{\xi,\eta}$) there are three modes, the AFMR mode M_1 and the two rare-earth modes $R_{3,4}$. Just as in the Γ_{24} phase, one of these (R_3) interacts weakly with M_1 and R_4 . The corresponding frequencies are therefore determined by the same equations as in the Γ_{24} phase, in which we must put $|G_x| = 1, G_z = 0, \cos \psi = 1$.

In the absence of dissipation we obtain from (21) for the resonance frequencies

$$\omega_{\pm}^2 = \frac{1}{2} (\omega_{10}^2 + \omega_{20}^2) \pm \Delta, \quad (27)$$

where

$$\Delta^2 = \Delta_0^2 + \omega_{12}^4, \quad \Delta_0 = \frac{1}{2} (\omega_{10}^2 - \omega_{20}^2),$$

and in the linear approximation in the damping constants δ_1 and Λ_1' we have for the corresponding linewidths

$$\Delta \omega_{\pm} = \frac{1}{2} \{ \Delta \omega_{10} + \Delta \omega_{20} \pm [\Delta \omega_{12}^2 + \frac{1}{2} (\Delta \omega_{10} - \Delta \omega_{20}) (\omega_{10}^2 - \omega_{20}^2)] / \Delta \}. \quad (28)$$

Let us analyze, on the basis of (21)–(28), the observed behavior of the AFMR and R modes in HoFeO_3 . In the Γ_4 phase the behavior of the M_1 and R_4 modes is determined by their interaction ($\omega_{12}^2 \sim \omega_{ex} \omega'_{ex} \sim \Delta_{ex}^2 / T$), which increases as T is lowered. As a result, the frequency $\omega_4^2(R) = \omega_-^2 \approx \omega_R (\omega'_R - \omega_{ex} \omega'_{ex} / \tilde{\omega}_{ac}^0)$ of the lower mode R_4 is lowered as $T \rightarrow T_1$ and vanishes at the point T_1 , while $\omega_1^2(\text{Fe}) = \omega_+^2 \approx \omega_E \tilde{\omega}_{ac}^0 + \omega_R \omega'_R$ remains finite.

In the low-temperature phase Γ_2 , conversely, the interaction of the AFMR and R modes influence little the frequencies even in the region of their crossing, since it is determined only by the isotropic R–Fe interaction and not by the enhanced Fe–Fe exchange (ω_E) [see Eq. (23)]. In this case the strong temperature dependence of the AFMR frequencies is determined by the corresponding effective anisotropy constants $K_{ca,cb}$ (14) renormalized by the R–Fe interaction: $\omega_{1,2}^2(\text{Fe}) \approx \gamma \omega_E K_{ca,cb} / M_0$. The temperature dependence of the effective anisotropy constant K_{ab} determines also the behavior of the strongly relaxing frequency of the M_2 mode in the phases Γ_4 and Γ_{24} .

According to (24) and (25), the interaction of the M_1 and R_4 modes in the canted phase Γ_{12} hardly differs from that in the Γ_2 phase, but for the M_2 and R_4 modes it increases strongly because of the appearance, in ω_{12} , of terms proportional to $\omega_R \omega_E \omega_{ex} \omega'_{ex}$, and determined by the exchange-enhanced anisotropic R–Fe interaction. Strong hybridization of the M_2 and R_4 modes takes place therefore in the interval T_2 – T_4 and increases the difference between their frequencies.

A general law governing the behavior of the AFMR-mode linewidths is their noticeable decrease (by 3–5 times) when T is lowered from 300 to 4.2 K, on the background of which are observed strongly pronounced anomalies (spikes) in the spin-reorientation region (40–60 K), and also a small increase in the region where the AFMR- and R-mode frequencies cross at $T \sim 30$ and 40 K. All these anomalies are due to the interaction and hybridization of the AFMR and R

modes. This hybridization is most strongly pronounced in the transition into the Γ_{12} phase at the point $T = T_3$ for the M_2 and R_4 modes, and is accompanied by a strong increase of the M_2 -mode linewidth $\Delta \nu_2(\text{Fe})$ and by a decrease of the R_4 -mode linewidth $\Delta \nu_4(\text{Fe})$ (Fig. 2). In the other canted phase (Γ_{24}) a similar behavior is exhibited by the interacting modes M_1 and R_4 : a strong increase of $\Delta \nu_1(\text{Fe})$ is observed in the T_2 – T_1 interval (Fig. 2). This picture of the behavior of the linewidths of strongly interacting AFMR and R modes is described by expression (28) (Fig. 2) at $\Lambda_1' = 10^{-4}$ (the remaining parameters are given in Sec. III.4 and in the table).

The situation is different for the weakly interacting mode pairs M_2, R_4 and M_1, R_3 in the Γ_2 phase. In this case the presence of finite linewidths alters qualitatively the behavior of the AFMR and R modes in the region of their frequency crossing at $T \approx 30$ K and $T \approx 40$ K. Analysis shows that as a result of the strong relaxation in the R subsystem at relatively weak mode interaction the solutions of Eq. (21) show no mode repulsion in the region where the real parts of the frequencies are equal ($\text{Re } \omega_1 = \text{Re } \omega_2$), since in the complete 3D space $\text{Re } \omega, \text{Im } \omega, T$ they are separated by a relatively large distance determined by the difference between their imaginary parts. This is just the situation for the mode pairs M_2, R_4 and M_1, R_3 in the Γ_2 phase and for M_1, R_3 in the Γ_{12} phase. In the transmission spectra this is manifested as passage of a narrow AFMR mode through a broad R mode with change of temperature. In the calculation of the parameters of the indicated modes in these phases we have therefore neglected their interaction (the frequencies of infinitesimally narrow modes should repel one another, as shown in Fig. 1 by the dashed line for the modes M_1 and R_2 at $T \approx 40$ K).

Let us discuss the behavior of the mode contributions that range, as seen from Fig. 3, over several orders of magnitude. We shall not present all the exact but unwieldy equations for the contributions used in the numerical calculations (Fig. 3) (see Ref. 35 for details), and confine ourselves mainly to a qualitative treatment. In the Γ_2 phase the contributions $\Delta \mu_y^{(1)}(\text{Fe})$ and $\Delta \mu_x^{(2)}(\text{Fe})$ of the AFMR modes M_1 and M_2 , which interact weakly with the R modes, are determined by the transverse susceptibility of the Fe subsystem and are equal to $\Delta \mu_y^{(1)}(\text{Fe}) \approx \Delta \mu_x^{(2)}(\text{Fe}) \approx 4\pi \chi_{\perp} = (7 - 8) \cdot 10^{-4}$. At a density $\rho = 8 \text{ g/cm}^3$ and at $M_0 = 103.8 \text{ G} \cdot \text{cm}^3/\text{g}$ this yields $\chi_{\perp} = M_0 / 2H_E = (0.7 - 0.8) \cdot 10^{-5} \text{ cm}^3/\text{g}$ and

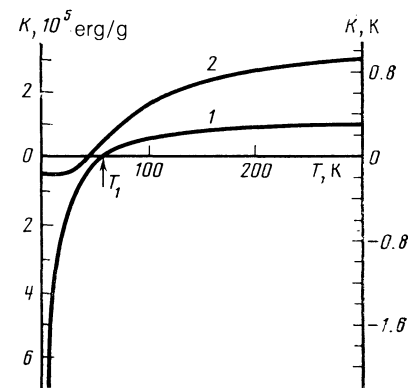


FIG. 5. Temperature dependences of the effective anisotropy constants in HoFeO_3 : 1— K_{ac} , 2— K_{ab} .

$H_E = (7.4 - 6.5) \cdot 10^6$ Oe, which agrees with $H_E = 6.4 \cdot 10^6$ Oe for YFeO_3 (Ref. 33). The same estimate holds also for the AFMR mode contributions $\Delta\mu_y^{(1)}(\text{Fe})$ and $\Delta\mu_x^{(2)}(\text{Fe})$ in the Γ_4 phase.

The strong growth of the contribution $\Delta\mu_z^{(1)}(\text{Fe}) = 4\pi\chi^{\text{rot}}$ of the soft mode M_1 in the Γ_{12} phase, observed as $T \rightarrow T_2$ (Fig. 3c), is due to the divergence of the rotational susceptibility $\chi_z^{\text{rot}} = (m_z^0)^2/K_{ca}$, since $K_{ca} \propto \omega_{ca}$ decreases strongly as $T \rightarrow T_2$. On the contrary, for the same mode M_1 in the Γ_4 phase the contribution $\Delta\mu_x^{(1)}(\text{Fe})$, which is also connected with the rotation susceptibility, decrease as $T \rightarrow T_1$ to a value

$$\Delta\mu_x^{(1)}(\text{Fe}) \approx 4\pi\chi_x^{\text{BP}}(1 - \varepsilon_1)^2/(1 + \varepsilon_2)^2,$$

where

$$\chi_x^{\text{rot}} = \frac{(m_x^0)^2}{K_{ac}^0}, \quad \varepsilon_1 = \frac{N\mu_x}{m_x^0} \frac{\omega_{ex}'\omega_R}{\omega_B\tilde{\omega}_{ac}^0},$$

$$\varepsilon_2 = \frac{\omega_R\omega_R'}{\omega_B\tilde{\omega}_{ac}^0}.$$

This is due to the strong interaction of the M_1 mode with the soft R_4 mode whose contribution $\Delta\mu_x^{(4)}$ diverges as $T \rightarrow T_1$: $\Delta\mu_x^{(4)}(\text{R}) \approx 4\pi(\chi_x^{\text{R}})_{\perp}\omega_R'/\tilde{\omega}_R \rightarrow \infty$, where $\tilde{\omega}_R = \omega_R - \omega_{ex}\omega_{ex}'/\tilde{\omega}_{ac}^0 \rightarrow 0$ as $T \rightarrow T_1$ and $(\chi_x^{\text{R}})_{\perp}$ is defined in (18).

We note finally the strongly pronounced anomalies of the contributions $\Delta\mu_x^{\pm} = \Delta\mu_x^{(4,2)}$ of the modes M_2 and R_4 at the point T_3 , which are connected with the new Γ_2 - Γ_{12} phase transition. The observed strong growth of the contribution of the low-lying mode M_2 and, on the contrary, the decrease of the contribution of mode R_4 , are explained by the strong hybridization of these modes on going into the phase Γ_{12} . The behavior of these contributions is well described by the equation

$$\Delta\mu_x^{\pm} = (4\pi\gamma f_0 n^{\mp}\omega_R/\omega_{\pm}^2 M_B) \{ [N\mu_x \cos \psi \mp (m_x^0\omega_B\omega_{ex}G_y^2 + M_0\omega_{bc}^0\omega_{ax})/(\Delta \mp \Delta_0)]^2 + \omega_{\pm}^2 G_y^2 (M_0\omega_{ex} - m_x^0\omega_{ax})^2/(\Delta \mp \Delta_0)^2 \},$$

(29)

where $n^{\pm} = (\Delta \pm \Delta_0)/2\Delta$, while Δ , Δ_0 , and ω_{\pm} are determined by (27) with $\delta_1 = \Lambda_1' = 0$. In addition, at the point T_3 the contribution $\Delta\mu_x^- = \Delta\mu_x^{(2)}(\text{Fe})$ of the soft mode M_2 undergoes a jump due to the appearance in the Γ_{12} phase of an additional rotation susceptibility $\Delta\mu_x^- = 4\pi(\chi_1 + \chi_{x1}^{\text{rot}})$ as $T \rightarrow T_3^+$ and $\Delta\mu_x^- = 4\pi\chi_1$ as $T \rightarrow T_3^-$, where

$$\chi_{x1}^{\text{rot}} = [m_x^0 + N\mu_x(\omega_{ex}'/\omega_R') \cos \psi]^2/2\tilde{K}_2, \quad \tilde{K}_2 = K_2 + K_2' - 2K_2''.$$

The modes M_1 and R_1 undergo also in the second canted phase (Γ_{24}) a hybridization manifested by an observable growth of the M_1 -mode contribution $\Delta\mu_x^{(1)}(\text{Fe})$ described by an equation similar to (29).

Our numerical calculations, based on (21)–(29), of the resonance frequencies, linewidths, and mode contributions have accounted well for the experimental results (Figs. 1–3), comparison with which yielded the parameters, listed in the table, of the principal magnetic interactions in HoFeO_3 . The table shows for comparison also some properties of the Ho and Fe subsystems from Refs. 19, 33, and 34. Note the good agreement between the obtained parameters that describe the Ho^{3+} ground quasidoublet, on the one hand, and the data of Ref. 19, on the other. The obtained HoFeO_3 properties have made it possible to calculate the $K_{ac,ab}(T)$ depen-

dences (Fig. 5) and determine the actual thermodynamic path (dash-dot in Fig. 4) along which the OPT Γ_4 - Γ_{24} - Γ_{12} - Γ_2 are realized.

IV. CONCLUSION

Our investigations of the high-frequency magnetic properties of HoFeO_3 have established the fine structure of the spin reorientation in this orthoferrite and revealed the main regularities of the dynamics of orientational transitions and the role played in it by the R subsystem. The observed anomalies of the frequencies, linewidths, and contributions of the AFMR and R modes at $T_1 = 58 \pm 2$ K, $T_2 = 51 \pm 1$ K, and $T_3 = 39 \pm 2$ K lead to the conclusion that a new canted phase $\Gamma_{12}(G_{y,z}, F_x)$ is realized in the interval T_2 - T_3 in HoFeO_3 , and that the spin reorientation is via three OPT Γ_4 - Γ_{24} - Γ_{12} - Γ_2 , i.e., the vector \mathbf{G} is rotated in two planes, first in the ac plane (Γ_{24}) and next in the bc plane (Γ_{12}).

Two contributions to the magnetic-anisotropy energy, due to the R-Fe interaction, have been revealed and determine the observed OPT pattern. The first is a Zeeman contribution due to the anisotropy of the exchange splitting of the Ho^{3+} ground quasidoublet, and the second a Van Vleck contribution due to displacement of the gravity center of the quasidoublet on account of an admixture of excited states. It is precisely the latter which causes the deflection of the vector \mathbf{G} from the ac plane.

Numerical calculations of the resonance frequencies, linewidths, and mode contributions to the static magnetic permeability describe well the experimental data and confirm the proposed spin-reorientation mechanism. The principal parameters of the magnetic interactions in HoFeO_3 have been determined and the temperature dependences of the anisotropy constants obtained.

As shown by a theoretical analysis (see also Ref. 35), the dynamic properties of orthoferrites in OPT depend substantially on the ratio of the R-mode frequencies determined by the splitting of the ground doublet (multiplet) of the REI and the natural AFMR frequencies of the Fe subsystem. If the AFMR frequencies are lower than those of the R modes, they are softened, and furthermore at both spin-reorientation boundaries, as for example in TmFeO_3 (Ref. 5). If, however, the R modes are lower, as in the case of HoFeO_3 , the picture becomes qualitatively different and is made complicated by the interaction of the AFMR and R modes and by the presence of soft modes of various types. Thus, in HoFeO_3 in the high-temperature phase at T_1 , the soft mode is the rare-earth mode R_4 , and the frequency of the AFMR M_1 mode interacting with it remains finite. In the low-temperature phases, conversely, the AFMR modes softened at T_3 and T_2 are the M_2 and M_1 , respectively, which interact weakly in this case with the R modes. The cause of this difference of the OPT dynamics at T_1 and $T_{2,3}$ is the strong anisotropy of the exchange splitting of the REI ground quasidoublet in the high- and low-temperature phases. The picture considered explains the anomalous behavior of the AFMR frequencies for OPT also in other orthoferrites (TbFeO_3 , ErFeO_3 , YbFeO_3), which have, just as HoFeO_3 , low-lying resonance R modes.

¹⁾ Allowance for the longitudinal oscillations, which requires a separate analysis, may turn out to be important in the immediate vicinity of the

OPT points, where interaction of the relaxation and soft resonance modes is possible.^{15,16,32}

- ¹K. P. Belov, A. K. Zvezdin, A. M. Kadomtseva, and R. Z. Levitin, *Oriental Transitions in Rare-Earth Magnets* [in Russian], Nauka, 1979.
- ²R. C. Le Craw, R. Wolf, E. M. Georgy, *et al.*, *J. Appl. Phys.* **39**, 1019 (1968).
- ³K. B. Aring and A. J. Sievers, *ibid.* **41**, 1197 (1970).
- ⁴V. I. Ozhogin, V. G. Shapiro, K. G. Gurtovoi, *et al.*, *Zh. Eksp. Teor. Fiz.* **62**, 2221 (1972) [*Sov. Phys. JETP* **35**, 1162 (1972)].
- ⁵S. M. Shapiro, J. D. Axe, and J. P. Remeika, *Phys. Rev.* **B10**, 2014 (1974).
- ⁶V. G. Bar'yakhtar, I. M. Vitebskiĭ, and D. A. Yablonskiĭ, *Zh. Eksp. Teor. Fiz.* **76**, 1381 (1979) [*Sov. Phys. JETP* **49**, 703 (1979)].
- ⁷R. M. White, R. J. Nemanich, and C. Herring, *Phys. Rev.* **B25**, 1822 (1982).
- ⁸N. Koshisuka and K. Hayashi, *J. Magn. Magn. Mat.* **31-34**, 596 (1983).
- ⁹S. Venugopalan, M. Dutta, A. K. Ramdas, and J. K. Remeika, *Phys. Rev.* **B27**, 3115 (1983).
- ¹⁰A. M. Balbashov, A. A. Volkov, S. P. Lebedev, *et al.*, *Zh. Eksp. Teor. Fiz.* **88**, 974 (1985) [*Sov. Phys. JETP* **61**, 573 (1985)].
- ¹¹N. K. Dan'shin, N. M. Kovtun, and M. A. Sdvizhkov, *ibid.* **84**, 203 (1985) [**57**, 115 (1985)].
- ¹²I. E. Golovenchits and V. A. Sanina, *Zh. Eksp. Teor. Fiz.* **89**, 203 (1985) [*sic*].
- ¹³A. M. Balbashov, G. V. Kozlov, S. P. Lebedev, *et al.*, *Pis'ma Zh. Eksp. Teor. Fiz.* **43**, 33 (1986) [*JETP Lett.* **43**, 41 (1986)].
- ¹⁴N. K. Dan'shin, G. G. Kramarchuk, and M. A. Sdvizhkov, *ibid.* **44**, 85 (1986) [**44**, 107 (1986)].
- ¹⁵A. M. Balbashov, A. G. Berezin, Yu. M. Gufan, *et al.*, *Zh. Eksp. Teor. Fiz.* **93**, 302 (1987) [*Sov. Phys. JETP* **66**, 174 (1987)].
- ¹⁶A. M. Balbashov, Yu. M. Gufan, P. Yu. Marchukov, *et al.*, *ibid.* **94**, No. 4, 305 (1988) [*Sov. Phys. JETP* **67**, 821 (1988)]. *Pis'ma Zh. Eksp. Teor. Fiz.* **41**, 391 (1985) [*JETP Lett.* **41**, 479 (1985)].
- ¹⁷H. Schuchert, S. Hufner, and R. Faulhaber, *Z. Phys.* **B220**, 280 (1969).

- ¹⁸A. P. Malozemoff and R. L. White, *Sol. St. Comm.* **8**, 665 (1970).
- ¹⁹J. C. Walling and R. L. White, *Phys. Rev.* **B10**, 4748 (1984).
- ²⁰A. Apostolov and J. Sivardiere, *Compt. Rend.* **B268**, 208 (1969).
- ²¹K. P. Belov, A. K. Zvezdin, A. M. Kadomtseva, *et al.*, *Fiz. Tverd. Tela* (Leningrad) **19**, 259 (1977) [*Sov. Phys. Solid State* **19**, 149 (1977)].
- ²²A. M. Balbashov, A. Y. Chervonenkis, A. V. Antonov, *et al.*, *Izv. AN SSSR, Ser. Fiz.* **35**, 1243 (1971).
- ²³A. A. Volkov, Yu. G. Goncharov, G. V. Kozlov, *et al.*, *Prib. Tekh. Eksp.* No. 2, 236 (1984).
- ²⁴J. R. Shine, *Phys. Rev. Lett.* **20**, 728 (1968).
- ²⁵A. K. Zvezdin, V. M. Matveev, A. A. Mukhin and A. I. Popov, *Rare-Earth Ions in Magnetically Ordered Crystals* [in Russian], Nauka, 1985.
- ²⁶A. K. Zvezdin and A. A. Mukhin, Preprint No. 225, *Inst. Gen. Phys. USSR Acad. Sci.* 1986.
- ²⁷D. N. Zubarev, *Nonequilibrium Statistical Thermodynamics*, Consultants Bureau (1974).
- ²⁸V. P. Kalashnikov and M. I. Auslender, *Fiz. Met. and Metallov.* **44**, 710 (1977).
- ²⁹V. G. Bar'yakhtar, *Zh. Eksp. Teor. Fiz.* **94**, No. 4, 196 (1988) [*Sov. Phys. JETP* **67**, 757 (1988)].
- ³⁰A. P. Agafonov and A. S. Moskvina, *Fiz. Tverd. Tela* (Leningrad) **30**, 612 (1988) [*Sov. Phys. Solid State* **30**, 353 (1988)].
- ³¹S. A. Altshuler and B. M. Kozyrev, *Electron Paramagnetic Resonance in Compounds of Transition Elements*, Halsted, 1975.
- ³²V. G. Bar'yakhtar, I. M. Vitebskiĭ, and D. G. Pashkevich, *Fiz. Tverd. Tela* (Leningrad) **26**, 1786 (1984) [*Sov. Phys. Solid State* **26**, 1080 (1984)].
- ³³J. S. Jacobs, H. Burn, and L. M. Levinson, *J. Appl. Phys.* **220**, 1631 (1971).
- ³⁴A. A. Volkov, Yu. G. Goncharov, G. V. Kozlov, *et al.*, *Pis'ma Zh. Eksp. Teor. Fiz.* **39**, 140 (1984) [*JETP Lett.* **39**, 166 (1984)].
- ³⁵A. M. Balbashov, G. V. Kozlov, S. P. Lebedev, *et al.*, Preprint No. 97, *Inst. Gen. Phys. USSR Acad. Sci.*, 1988.

Translated by J. G. Adashko